GAIA: global astrometry from space at 10 μas level

D. Carollo, B. Bucciarelli, M. Gai, M. G. Lattanzi and S. Cesare*

Astronomical Observatory of Torino
Strada Osservatorio, 20 - 10025 Pino T.se (To) - Italy
**Alenia Spazio, C.so Marche, 31 – 10100 Torino - Italy*

Keywords: space instrumentation - astrometry – interferometry - data analysis

ABSTRACT

Based on the success of its previous astrometric space mission HIPPARCOS, the European Space Agency recommended the study of a cornestone mission named GAIA dedicated to astrometry, with the goal of 10 μas astrometric accuracy at magnitude V = 15. GAIA's direct output will be an extensive network of stellar distances, proper motions and positions throughout a significant fraction of the Galaxy, which would lead to important scientific results in major astronomy and astrophysics fields. In this paper the mission concept and feasibility study are outlined. Critical issues concerning instrumental calibrations versus scientific mission requirements are also addressed.

1. INTRODUCTION

GAIA is a preliminary concept for an astrometric mission of the European Space Agency (ESA) which should provide positions, proper motions, and parallaxes of some $5 \cdot 10^7$ objects, down to about V=15 mag, with an accuracy of better than **10 μas,** along with multi-color multi-epoch photometry of each object (Lindegren & Perrymann, 1996) GAIA performs global astrometry, i.e. the entire celestial sphere is observed, and the results refer to a unique and well-defined reference system. This implies the determination of absolute parallaxes and of a dense and undistorted optical reference frame for positions and proper motions.

From a technical viewpoint, the main characteristics of the GAIA mission concept can be summarized as follow:

- geostationary orbit or libration orbit around the Lagrangian point L2 in the Sun-Earth system;
- continuous scanning of the celestial sphere along instantaneous great circles, with simultaneous observations of two sky regions separated by a wide *basic angle* ($54°$);
- wide field of view (FOV ~1 $\deg^2$) and high angular resolution in the scanning direction;
- the spacecraft rotation and precession, along with the orbit of Earth around the Sun, combine to give complete sky coverage;
- each star is observed several times during the mission allowing a complete determinations of the astrometric stellar parameters. All the parameters are in principle determined in a single, global adjustment procedure;

The satellite could be launched in 2009, with vectors Arianne 5 in a dual launch, and the expected nominal mission lifetime is 5 years.

1.2 General scientific objectives

GAIA will provide an enormous quantity of data of extremely accurate astrometry and photometry from which all branches of astrophysics will benefit, in particular in the field of the physics and evolution of individual stars and of the whole Galaxy. This process has began already with the results of the ESA astrometry mission HIPPARCOS launched in June '89. However, while HIPPARCOS could probe less than 0.1 % of the volume of the Galaxy by direct distance measurement, GAIA will encompass a large fraction of the Milky Way system within its parallax horizon, including much of the Galactic halo, and even touching on the nearest companion galaxies such us the Magellanic Clouds.

We can summarize the scientific objectives as follow:

- establishment of an optical reference system by means of an accurate set of reference directions for dynamical interpretations of the motion of the Earth and other planets and of the Milky Way;
- physics and evolution of individual stars;
- dynamics of stellar systems;
- formation and evolution of the Galaxy;
- distance determination of the nearby Cepheydes and RR-Lyrae stars, fundamental to define the distance scale to nearby galaxies and cluster of galaxies;
- detection of extra-solar planets and brown dwarfs: in a volume of 200 pc of radius the number of stellar candidates is about 2-3 hundred thousand; up to this distance GAIA will be able to detect perturbations of Jupiter like planets (p=11.2 years, a= 5 AU), with probability larger then 50%;
- general relativity: possible detection of gravitational waves, and accurate (10^{-6}) measure of the parameter γ due to the Sun.

2. INSTRUMENT DESCRIPTION

The main task of the GAIA astrometric instrument is the measurement of angles between stars belonging to two widely separated sky regions. Basically, the instrument is composed by an optical part and a detection system (CCD sensor mosaic) placed on the focal plane.

The feasibility study has suggested two different configurations: the interferometric (with two apertures) and the monolithic option (single aperture). In the following we will concentrate on the former option.

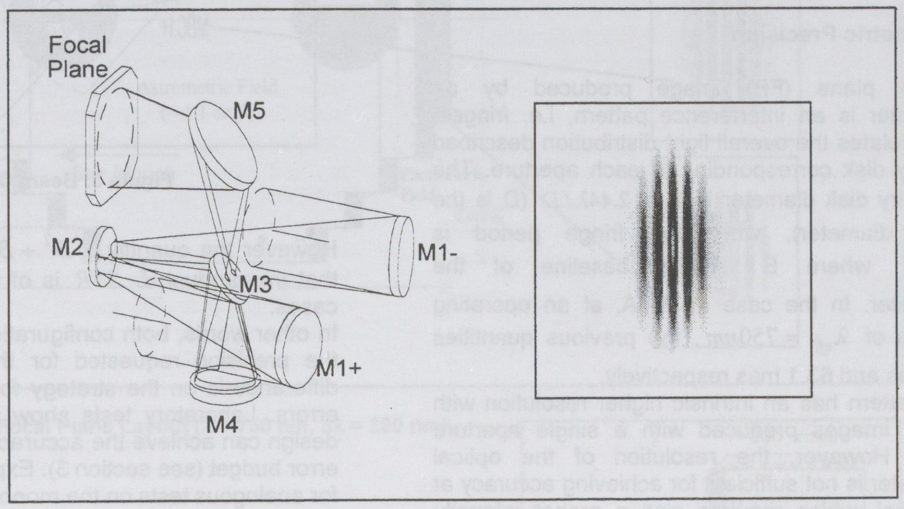

Figure 1: Optical interferometer configuration and star image on the focal plane

2.1 Interferometer Optical configuration

The Optical Instrument is constituted by two elements (Cesare, 1998):

- Korsch-type interferometer which produces star images on the focal plane with an intrinsic high spatial resolution in the along-scan direction.

- A beam combiner (BC) which endows the optical interferometer with two lines of sight.

The optical interferometer (figure 1) consists of two elliptic primary mirrors ($M1_+$, $M1_-$) with 0.65 m aperture and separated by a 2.45 m baseline, an hyperbolic secondary mirror M2, another elliptic mirror (M4), and two flat mirrors (M3, M5). The mirrors M2 to M5 are monolithic and lie on the optical axis of the interferometer.

The geometric features and the parameters of the telescope optical configuration are summarized in table 2.

Table 2: geometric features of GAIA telescope

Parameter	Value
Baseline	2.45 m
Aperture Diameter (≡ entrance pupil diameter)	0.65 m
Effective Focal Length	40 m
Overall field of view	1.4°×1.4°

One of the goals of GAIA is to determine "absolute parallaxes" of the stars, i.e. parallaxes which are independent of distance and motion of background stars. To achieve this goal, GAIA must be able to perform measurements of the separation angle between stars belonging to widely separated sky regions (i.e. of stars with very different *parallax factors*). In the present design this capability is achieved by endowing the telescope with two different lines of sight (LOS1 and LOS2) separated by a wide angle (the *basic angle*, BA) by means of an optical system called "beam combiner" .

The beam combiner (figure 3) consists of four flat mirrors placed in front of the primary mirrors. They intercept the light coming from two directions separated by a basic angle of 54° (which is defined by the angle between the normals to the four mirror surfaces) and reflect it towards the interferometer apertures.
This solution is similar to that adopted in the HIPPARCOS mission and the main benefits are:

- The BC constitutes a physical realisation of the basic angle, i.e. one of the fundamental quantities which affect the accuracy of the star position, parallax and proper motion determination. At the same time, the BC allows to identify a conceptually simple way of monitoring and controlling its stability, i.e. through the control of the relative orientation of the BC mirrors.

- Most of the effect (shift of the fringe pattern) produced by the movements of the optical interferometer mirrors is common to both FOVs. Therefore, since the basic measurements are angular separations of the stars belonging to different FOVs, which are routed into the same instrument by the beam combiner, it is possible to relax the measurement/control requirements of the relative position/orientation of the telescope mirrors.

2.2 Astrometric Precision

The focal plane (FP) image produced by an interferometer is an interference pattern, i.e. fringes, which modulates the overall light distribution described by the Airy disk corresponding to each aperture. The principal Airy disk diameter is $T_A = 2.44\lambda / D$ (D is the apertures diameter), while the fringe period is $T_y = \lambda / B$ where B is the baseline of the interferometer. In the case of GAIA, at an operating wavelength of $\lambda_{eff} = 750nm$, the previous quantities are 581 mas and 63.1 mas respectively.
A fringe pattern has an intrinsic higher resolution with respect to images produced with a single aperture telescope. However, the resolution of the optical interferometer is not sufficient for achieving accuracy at 10 μas level, which requires also a proper intensity (high number of photons).
As we have seen, the feasibility studies suggest two different options for the optical configuration. In both cases, the lower limit for the location error in the along scan direction, for the single measure, depends on the signal to noise ratio (SNR) and the geometric characteristics of the telescope, precisely:

$$\sigma \geq F \frac{\lambda}{L \cdot SNR}, \qquad SNR \leq \sqrt{N} \qquad (1)$$

where for the single aperture option L = D (aperture diameter), while for the interferometric option L = $\sqrt{D^2 + B^2}$, N = number of photons, and F is a parameter related to the geometry of the telescope and the detection system.
The product $L \cdot SNR$ should in general be maximized in order to obtain the precision requested for GAIA taking into account the various constraints on size, mass and complexity of the satellite payload.
For example, the monolithic option has a greater aperture (L = 1.7 m) compared to the interferometer (D = 0.65 m), therefore the signal to noise ratio is higher for the former.

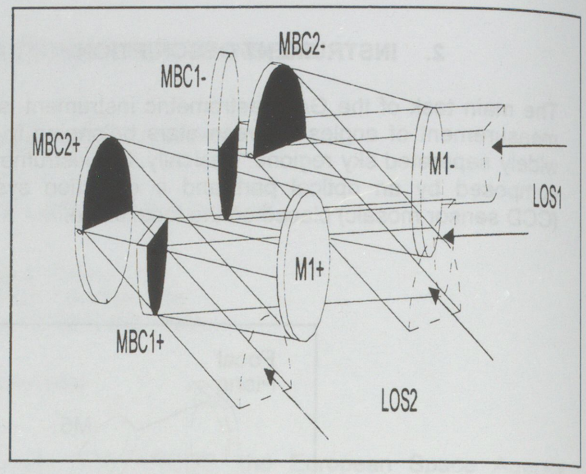

Figure 3: Beam Combiner

However the quantity $\sqrt{D^2 + B^2}$ is greater than L, so that the product $L \cdot SNR$ is of the same order in both cases.
In other words, both configurations achieve in principle the precision requested for the GAIA mission. The difference is on the strategy for controlling systematic errors. Laboratory tests show that the interferometric design can achieve the accuracy value allocated in the error budget (see section 3). Experiments are underway for analogous tests on the monolithic configuration.

2.3 Focal plane and detection system

The detection system consists of a CCD (Charge Coupled Device) mosaic placed on the focal plane of the telescope (Cesare, 1998).
The detection area is functionally subdivided in three parts (figure 4):

- the Astrometry area, placed in the central part of the focal plane where the fringe visibility is higher, is dedicated to the very accurate measurement of the along-scan coordinate of stars up to the 18th magnitude (single-exposure S/N ratio > 4).

- the Photometry area, constituted by two zones ('preceding' and 'following' Photometry areas) placed at the two sides of the Astrometry area and covered by a set of pass-band filters, is dedicated to the measurement of the star light flux in different spectral regions (U, B, V, Rc, Ic, etc..)

- the Star Mapper, constituted by two "strips" placed at the outer edges of the FP in the scan direction, dedicated to the attitude determination as well as to photometric measurements.

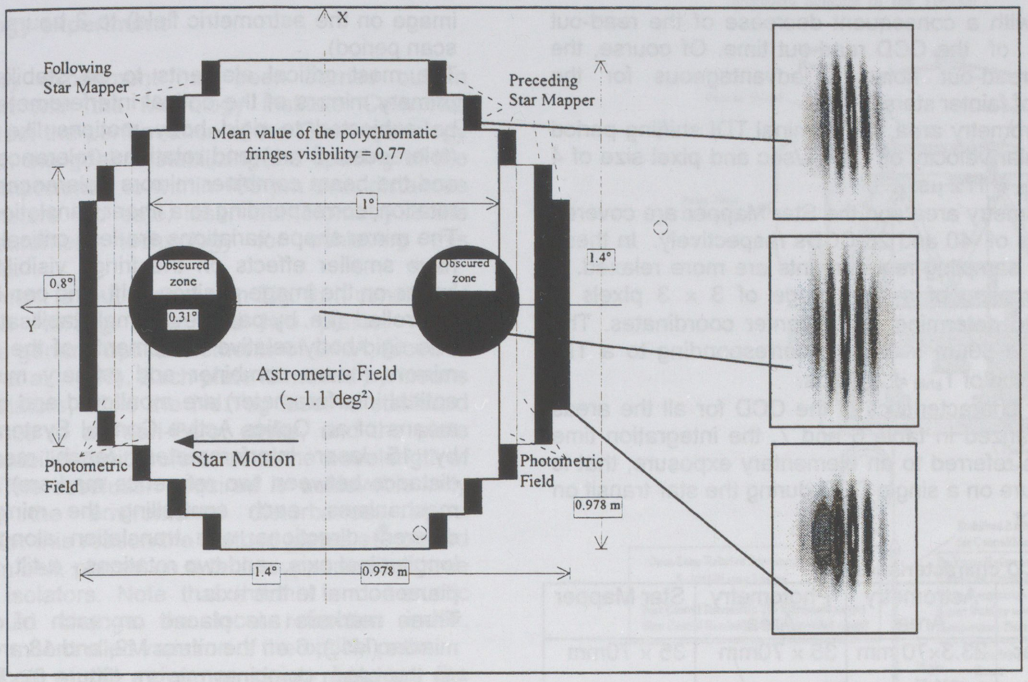

Figure: 4: Focal Plane Layout (λ = 750 nm, $\Delta\lambda$ = 200 nm)

The preceding Star Mapper views all the stars during the scan motion of the satellite, and implements different and important functions, such as:

- detection of the presence of each star entering the FP, up to a limiting magnitude V = 20
- estimation of the times at which the star will transit on the successive FP zones (i.e., the preceding Photometry area, the Astrometry area, the following Photometry area and the following Star Mapper); transmission of these data to the relevant detector control electronics
- determination of the position occupied by the star on the Star Mapper at a given time

This area of the focal plane allows to perform a significant data reduction at the detector level. In fact using the information from the preceding Star Mapper, it is possible to read out just the detector zones in which the presence of a star is expected, discarding the empty pixels.

All the CCDs are operated in Time Delay Integration (TDI) mode, which consists in shifting all the charges of a vertical line (row) to the next row at a velocity equal to the apparent star velocity (figure 5). This CCD operation mode is implemented to accumulate charges for a sufficient time (established by the along-scan pixel size), at the same time avoiding the image smearing otherwise caused by the continuous change of the telescope line of sight.

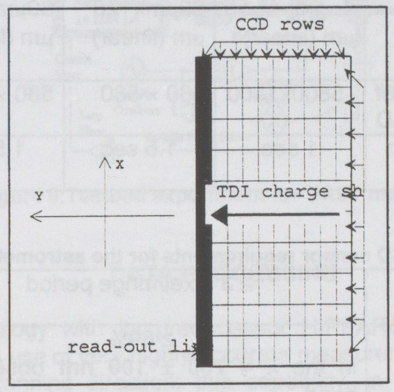

Figure 5: TDI mode

The apparent star velocity is different from chip to chip because of the residual telescope field distorsion. Therefore, the TDI line shift must be clocked by independent oscillators.

The Astrometry area is covered by a mosaic of 632 CCDs of three different sizes. Each CCD is made of rectangular pixels with size 4×50 μm (optimized for λ = 750 nm).

The interference fringes are present only in the along scan direction, due to the telescope optic design, while in the cross scan direction, the photons distribution follows the diffraction pattern. Given that each fringe must be sampled with at least 3 pixels to properly reconstruct the signal, the along scan direction is characterized by the smaller pixel dimension.

In the cross-scan direction the star image can be sampled with a much lower resolution: a single sample of the Airy disk of the image is sufficient. In this direction the linear size of the Airy disk is 226 mm, which correspond to ~ 5 pixels. To obtain a single sample, a technique for the image acquisition named *binning* has been proposed, which consists in building a macropixel made of 5 pixels containing the full Airy disk. In such a way, the number of pixels processed is

reduced, with a consequent decrease of the read-out noise and of the CCD read-out time. Of course, the reduced read-out noise is advantageous for the detection of fainter stars.
In the Astrometry area, the nominal TDI shifting period (with angular velocity of 120 as/sec and pixel size of 4 mm) is $T_{shift} \approx 172$ μs.
The Photometry area and the Star Mapper are covered by mosaics of 40 and 28 CCDs respectively. In these areas, the sampling requirements are more relaxed. A typical sampling of a star image of 3 × 3 pixels is sufficient to determine photocenter coordinates. The pixel size is 60μm × 120μm, corresponding to a TDI shifting period of $T_{shift} \approx 2580$ μs.
The major characteristics of the CCD for all the areas are summarized in table 6 and 7, the integration time reported is referred to an elementary exposure, that is the exposure on a single CCD during the star transit on the detector.

Table 6: CCD characteristics

	Astrometry Area	Photometry Area	Star Mapper
CCD linear size	23.3×70 mm	35 × 70mm	35 × 70mm
Pixel size	4 μm × 50 μm (linear)	60μm×120 μm (linear)	60μm×120 μm (linear)
Number of pixel in CCD	~5800×1400	580 × 580	580 × 580
Integration time	1 sec	1.5 sec	1.5 sec

Table 7: CCD sensor requirements for the astrometry area

Image sampling	≥ 3 pixel/fringe period
Quantum efficiency	≥ 60% in the λ = 750 ± 100 nm observation band
Read-out-noise	≤ 3 e^-
Charge transfer inefficiency	≤ 10^{-6}

3. METROLOGY

The metrology for the GAIA interferometric instrument is one of the most crucial issues to the success of the mission.
The optical part of the instrument must be kept stable essentially for two reasons: formation and persistence of the interference fringes, and stabilization of the basic angle (Cesare, 1998).
Concerning the former, the fringe visibility must be always close to its nominal value (visibility loss ≤ 5%) across the astrometric field. The second reason is nevertheless crucial, in fact while the basic angle between two lines of sight needs to be controlled within 5 μas, the stability of the relative position of star images in two different FOVs is relaxed to 10 μas to take in to account geometric field distorsion variability, in the time scale from 0.75 sec (minimum integration time of a star image on the astrometric field) to 3 hours (great circle scan period).
The most critical elements to be stabilised are the primary mirrors of the optical interferometer which can be subjected to rigid body motions like translations (tolerances: 5 nm) and rotations (tolerances: 1.8 nrad) and the beam combiner mirrors (tolerances: 17 prad in rotation, corresponding to a linear translation of 6 pm).
The mirror shape variations are less critical, in fact they have smaller effects on the fringe visibility loss, and hence on the image position shift, and can be passively controlled (i.e. by passive thermal stabilisation).
The rigid-body relative movements of the most critical mirrors (beam combiner and primary mirrors of the optical interferometer) are monitored and controlled by means of an Optics Active Control System composed by 15 laser interferometers (each measuring the distance between two reference markers) and 5 tip-tilt mechanisms, each controlling the mirror in three different directions: one translation along the mirror longitudinal axis, and two rotations - α-tilt, β-tilt - of the plane normal to this axis.
Three markers are placed on each of the primary mirrors ($M1_{\pm}$), 6 on the mirror M2, and 18 are distributed on the beam combiner mirrors (figure 8). The markers are attached to the mirrors through optical contact.
The laser interferometers monitor the distance variation between reference markers (caused by rigid-body movements of the mirrors) and the tip-tilt mechanism moves the "active mirrors" to compensate the distance variations. Moreover, several tests and simulations have demonstrated that, as a consequence of the distance control between the selected reference points, also the fringe contrast, the star relative position and the basic angle are also kept under control.
Error analyses have shown that the measures of both absolute and relative distances must be performed by laser metrology with the following accuracy: $\delta s/s = 4 \cdot 10^{-9}$ 1σ (relative error for the absolute distance measurements), and $\delta s/s = 8 \cdot 10^{-12}$ 1σ (relative error on distance variation measurement). In order to attain these results the laser frequency variation must be stable at $\delta\nu/\nu < 8 \cdot 10^{-12}$ 1σ over 0.75 s ÷ 3 h time scales.

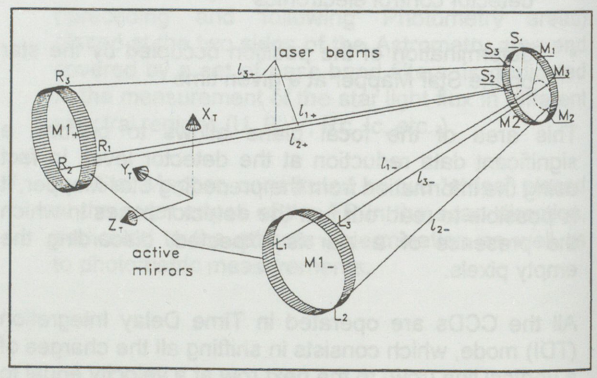

Figure 8: Position of the reference markers (L_i, M_i, R_i, S_i,) on the optical interferometer mirrors

3.2 Metrology experiment

A laboratory experiment has been carried out in collaboration with the Metrology Institute *Colonnetti* (Torino) to test the performance of the GAIA metrology system, with the goal of stabilizing the spacing of the optical components to within 100 pm over distances of a few meters. To date, laser interferometry is the best measurement technology for achieving this performance.

The experiment layout is shown in Fig. 9. It consists of a stabilized Nd:Yag laser and two plates, which simulate the generic optical elements of GAIA, faced at 0.5 m (Gai et al, 1997). Each plate is moved by means of piezotraslators, while the Nd:Yag laser is stabilized with reference to a Fabri-Perot cavity, and the plate spacing is stabilized with reference to the wavelength of this laser. The resolution required is achieveble only maintaining the enviromental disturbances at a minimum. For this reason the testbed plates are placed in a vacuum bell, placed on a table supported by three pneumatic isolators. Note that thermal and acoustic effects would change the local refraction index, resulting in uncontrolled variation of the optical paths.

The distances of the reference points between the plates are measured by means of Fabry-Perot interferometers, and actively controlled to within 100 pm (picometers). In a Fabry-Perot interferometer the monochromatic light is channeled through a pair of parallel half-silvered glass plates, producing circular interference fringes. One of the glass plates is adjustable, enabling the separation of the plate to be varied. The wavelength of the light can be determined by observing the fringes while adjusting the separation.

The basic Nd:Yag laser is a ligthwave mod. 146 operating at λ=1.064 μm, with narrow emission and a wavelength stability of ~ 1 part on 10^8, for a three hours observation time. The laser is stabilized with reference to an optical cavity, with a ultra-low thermal expansion coefficient, by means of the Pound-Drever method (reference material : ULE®, CTE = 10^{-8} /K).

The required reference cavity temperature stability is $\delta T < 8 \cdot 10^{-4}$ K 1σ over 0.75 s ÷ 3 h time scales.

The absolute distance measurement principle is the following: the absolute distance (s) between two markers is obtained from the frequency variation measurements $\Delta\nu$, in mathematical form we have:

$$\Delta\nu = \frac{c}{2s} \qquad (2)$$

where c is the light velocity.

The requirements for GAIA correspond to distance stabilization constraints to better then 2 pm.

The experiment lead to very interesting results: digital control kept the average distance variations between the mirror pair at the level of 2pm (1σ). Moreover, digital control guarantees to maintain these performances unaltered during longer time scales like in the GAIA system (3 hours).

The sub-nanometric optics stabilization is then demonstrated.

Simplified Scheme of the Testbed

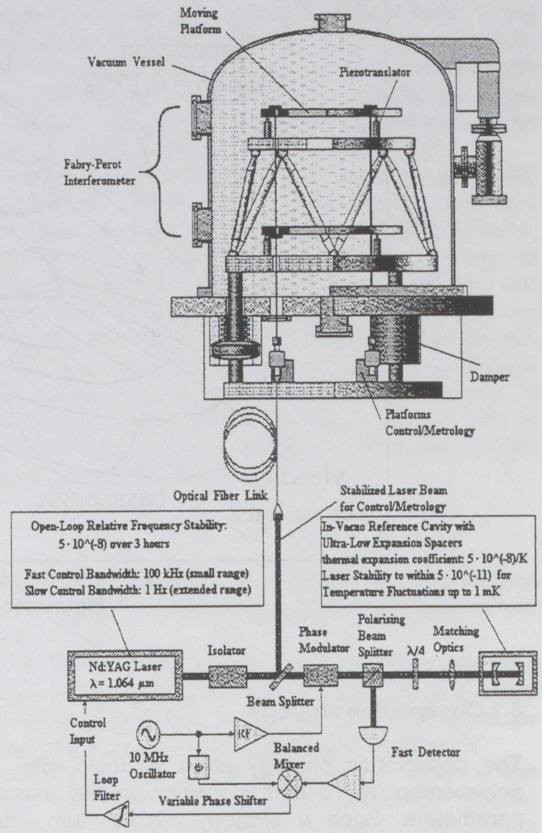

Figure 9:Testbed experiment for GAIA metrology

DATA PROCESSING

In analogy with its predecessor HIPPARCOS, GAIA makes use of very highly accurate measurements along the scanning direction; this capability, in conjunction with the peculiar scanning law according to which the same object is observed many times at different scanning orientation, allows to reconstruct the stellar astrometric parameters with a precision of a few micro-arcseconds. In principle, the problem is very much similar to that of HIPPARCOS, with the difference that the number of stars involved is ~ 10^4 times larger and the target error ~ 10^3 smaller.

Therefore, the data reduction task has to take into account all possible effects, both of physical nature as well as numerical, which can introduce an indetermination or a systematic error at the level of the sought for accuracy (Bucciarelli et al., 1997). We do not discuss here this kind of details; instead, we present an outline of the principles of the reduction strategy which will need to be further developed.

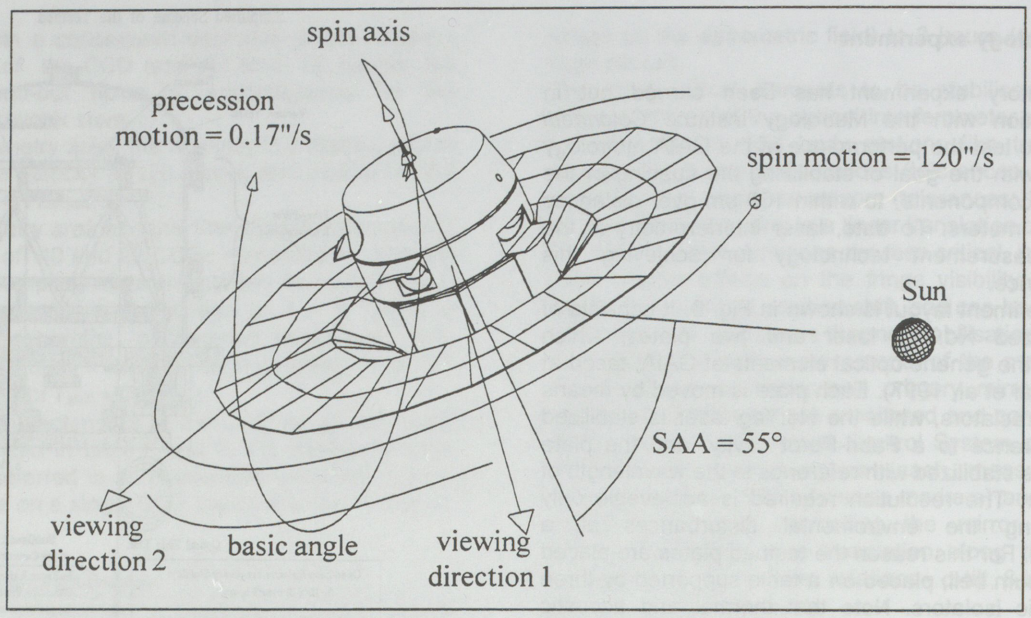

Figure 10: The GAIA nominal scanning law

4.1 Observation strategy

The observation strategy plays a basic role in the achievement of 10 mas accuracy on the astrometric parameters. Such a strategy is, in turn, strongly connected with the chosen scanning law, as it is explained in the following.

The attitude of the spacecraft follows a complex "revolving scanning" motion, called the *nominal scanning law*, which ensures a complete sky coverage over the lifetime of the mission and allows to reduce the thermal perturbations on the payload.

The spin direction is maintained constant at 55° angle with respect to the Sun direction, and rotates with angular velocity of 120 as/sec (120° for hour), and a period of 3 hours. The axis has a precession motion around the solar directions with constant precession rate = 0.17 arcsec/s (4.14 revolution/year). A pictorial representation of the satellite scanning law is given in figure 9.

A complete great circle in the sky is scanned in 3 hours by the instrument line of sight, and the closure conditions on the great circle allow accurate determination of the most critical geometrical instrument parameters (in particular the basic angle between the two viewing direction) with a time resolution corresponding to the spin period.

The path scanned on the sky in one year by one of the lines of sight of the Astrometric Instrument following the nominal scan law is shown in Figure 11.

As a star enters the preceding (or following) FOV, its interference fringe pattern is recorded on the main CCD field. Then, the first reduction step consists in using this fringe pattern to accurately determine the photocenter position of each stellar image with respect to the optical axis.

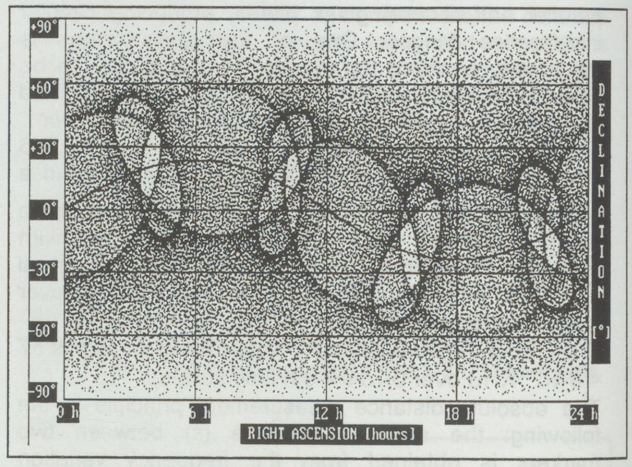

Figure 11: Path described in the sky by one line of sight in one year

4.2 Strategy of reduction

In order to formulate the observation equation we note that the GAIA measurement has a very high resolution in only one direction, i.e., that of the satellite instantaneous scanning velocity. Therefore, the measure of a star position as seen in the instantaneous FOV, neglecting deviations from flat-field geometry caused by instrumental effects, which nevertheless must be accurately calibrated, can be expressed by the following equation:

$$x_{ik} = \vec{r}_{ik} * \vec{E}_{ik} \qquad (3)$$

where x is the projection along the scanning direction of the star distance from the FOV center, $\vec{r}$ is the unit vector representing the geometric direction to the stellar

source, and $\vec{E}$ is the unit vector perpendicular to the optical axis, and directed along the instantaneous scanning velocity. The indices *i* and *k* refer to star *i* at time *k*, respectively.
In this context one assumes that both classical and relativistic apparent places effects are removed a priori from the observed star position. In particular, the vector $\vec{r}$ is a function of the 5 astrometric parameters which one wants to estimate, namely: $\vec{r} = \vec{r}(\alpha, \delta, \mu_\alpha, \mu_\delta, \pi)$, where α and δ are the stellar coordinates, μ_α, μ_δ are the stellar proper motions, and π the parallax.
In a more explicit form, the following vectorial expression holds:

$$r(t) = \vec{u}_b(T)[1 + \pi V_R(t-T)] + \pi \dot{\vec{u}}_b V_T(t-T) + \pi \vec{u}_{Sun}\rho(t) \quad (4)$$

where t is the epoch of observation, T the reference epoch, $\vec{u}_b = \vec{u}_b(\alpha,\delta)$ is the unit vector in the barycentric direction to the star, V_T and V_R are the star barycentric tangential and radial velocity (AU/year), $\dot{\vec{u}}_b = \dot{\vec{u}}_b(\mu_\alpha, \mu_\delta)$ is the unit vector in the direction of V_T, $\vec{u}_{Sun}$ is the unit vector Satellite-Sun, and ρ is the distance Satellite-Sun (AU).
In analogy with the HIPPARCOS mission, one of the key requirements of GAIA is the presence of two FOVs separated by a large angle. This peculiarity, which was originally devised in order to estimate absolute parallaxes by observing couples of widely separated stars, allows to easily reconstruct the arcs between stars simultaneously observed in the two FOVs. Therefore, the data reduction problem can be assimilated to that of a global network adjustment of arcs on the sphere, irrespective of the satellite attitude.
However, a correlation analysis performed on this model has shown that in the arc approach there is a non negligible correlation of about 0.5 among arcs having one end in common (Betti et al., 1983).
On the other end, one can abandon the concept of arcs and use the fact that the observations are made in two distinct directions separated by a large basic angle, in order to determine with sufficient accuracy the spin axis attitude at any instant of time.
In such an approach, the equation (3) is regarded as the *condition equation*, which is linearized as follow:

$$\delta x_{ik} = \delta \vec{r}_{ik} * \tilde{\vec{E}}_{ik} + \delta \vec{E}_{ik} * \tilde{\vec{r}}_{ik} \quad (5)$$

where $\delta \vec{E}_{ik}$ is forced to be in the scanning plane, and $\tilde{\vec{r}}_{ik}$, $\tilde{\vec{E}}_{ik}$ are zero-order approximations.

The along satellite velocity $\delta \vec{E}_k / \delta t$ can be modeled by a small number of parameters, as it is a very smooth motion, while the fact that the same stars are observed several times during the mission lifetime, gives the necessary redundancy to the linearized equation system.
Noting also that only a small number of attitude unknowns is linked in time, since there is a discontinuity every time the satellite path is actively corrected, the structure of the resulting normal matrix of the system of equations has a two-by-two block structure of the type:

$$A'A = \begin{vmatrix} B & V \\ V' & C \end{vmatrix}$$

where B and C are block-diagonal, and refer to astrometric and attitude unknowns respectively; V and its transpose V' come from the combination of both astrometric and attitude unknowns, and are therefore rather full matrices. Given the extremely large dimension of the system, numerical strategies must be explored in order to make the solution feasible.
Numerical experiments reported in Sansò et al. (1989) on simulated HIPPARCOS data showed that this system can be solved using a simple iterative scheme. First, the attitude is kept fixed and a solution is made for the stellar astrometric parameters only; then the star parameters are fixed, and the attitude is adjusted. The whole process is iterated until convergence is reached. With this scheme, even though only partial knowledge of the covariance of the estimated parameters is retained, the numerical complexity of the problem is drastically reduced since only the block-diagonal sub-matrices need to be inverted.

CONCLUSION

GAIA's feasibility studies have shown that this mission has the potential to perform global astrometry at the level of 10 μas.
Most of the studies carried out for GAIA are also relevant to the new generations of ground and space instrumentation, which make use of highly accurate interferometry as well as active control techniques.
Further development of the concepts addressed in this paper, regarding in particular detection system optimization, telemetry data throughput, and data reduction, are underway.

References

Betti B., Mussio L., Sansò F., 1983, in "The First FAST Thinkshop", ed. P.L. Bernacca, Padova University, pp. 281-298

Bucciarelli B, Lattanzi M., Spagna A., 1997, Proc. ESA Symp. Hipparcos Venice '97, Isola S. Giorgio, Venezia, Battrick B. ed., ESA Publ. Division, ESA SP-402, pp. 277-279

Cesare S., Active Pointing of Large Telescope & Attitude Measurement Transfer Systems, Final Presentation, SD-PB-AI-0301, October 14, 1998, ESTEC-Noordwijk

Gai M., Casertano S., Carollo D., Lattanzi M.G., 1998, Location Estimators for Interferometric Fringes, Publ. Astron. Soc. Pacific, 110, pp. 848-862

Gai M., Bertinetto F., Bisi M., Canuto E., Carollo D., Cesare S., Lattanzi M.G., Mana G., Thomas E., Viard T., 1997, GAIA Feasibility: Current Research on Critical Aspects, Proc. ESA Symp. Hipparcos Venice '97, Isola di S. Giorgio, Venezia Battrick B. ed., ESA Publ. Division, ESA SP-402, pp. 835-838

Lindegren L., M.A.C. Perrymann, 1996, A & AS, 116, 579

Sansò F., Betti B., Migliacci F., 1989, ESA SP-1111, Vol. 3, The Data Reduction, pp. 437-455